

# **A novel dendrimeric peptide with antimicrobial properties: *in vitro* characterization of SB056**

**Mariano A. SCORCIAPINO\*†, Giovanna PIRRI‡, Attilio V. VARGIU†, Paolo Ruggerone¶†, Andrea GIULIANI‡, Mariano CASU\*, Jochen BUERCK§, Parvesh WADHWANI§, Anne S. ULRICH§, Andrea C. RINALDI||<sup>1</sup>**

\* Department of Chemical Sciences, University of Cagliari, I-09042 Monserrato (CA), Italy

† CNR-IOM, UOS SLACS, c/o Department of Physics, University of Cagliari, Monserrato (CA), Italy

‡ Research & Development Unit, Spider Biotech S.r.l., I-10010 Collieretto Giacosa (TO), Italy

¶ Department of Physics, University of Cagliari, I-09042 Monserrato (CA), Italy

§ Karlsruhe Institute of Technology (KIT), Institute for Biological Interfaces (IBG-2), Institute of Organic Chemistry and CFN, Karlsruhe, Germany

|| Department of Biomedical Sciences and Technologies, University of Cagliari, I-09042 Monserrato (CA), Italy

## Supporting Material

### MATERIALS AND METHODS

#### Materials and Peptide's synthesis

A manual standard solid-phase peptide Fmoc (9-fluorenylmethoxy-carbonyl) strategy was employed, working under nitrogen flow. Amino acids and a NovaPEG Rink Amide resin (0.67 mmol/g) were purchased from Sigma-Aldrich-Fluka (St. Louis, MO, USA) and Novabiochem (Merck Chemicals Ltd., Nottingham, UK). Peptide synthesis grade *N,N*-dimethylformamide (DMF), *N*-methylpyrrolidone (NMP), trifluoroacetic acid (TFA), dichloromethane, diethyl ether and *O*-(Benzotriazol-1-yl)-*N,N,N',N'*-tetramethyluronium hexafluorophosphate (HBTU) were purchased from ChemImpex (Wood Dale, IL, USA) and Sigma-Aldrich. 1,2-Dimyristoyl-*sn*-glycero-3-phosphocholine (DMPC) and 1,2-dimyristoyl-*sn*-glycero-3-phospho-*rac*-(1-glycerol) sodium salt (DMPG) were from Sigma-Aldrich. All other reagents and solvents were purchased from Sigma-Aldrich at the highest available purity and were used with no further purification.

The monomeric linear peptide was synthesized with an amidated C-terminus [WKKIRVRLSA-NH<sub>2</sub>], and the dendrimeric SB056 was synthesized as a branched dimer on a lysine scaffold with an amidated lipidic tail ([WKKIRVRLSA]<sub>2</sub>-K-8Aoc-NH<sub>2</sub>, see Fig. 1). A manual standard solid-phase peptide Fmoc (9-fluorenylmethoxy-carbonyl) strategy was employed, working under nitrogen flow. Coupling reactions with Fmoc-protected amino acids were activated *in situ* using HBTU, 1-hydroxybenzotriazole (HOBt) and diisopropylethylamine (DIPEA) with the ratio HOBt/DIPEA/HBTU of 1/2/0.9. The branched lysine core was synthesized on the resin by using (Fmoc)<sub>2</sub>Lys-OH protected amino acid, and the first amino acid on the core was aminated with 8-aminooctanoic acid (8-Aoc). A sixfold excess of each Fmoc-protected amino acid was employed in every coupling step of the synthesis, and the following acid-labile protecting groups were used for reactive side chains: 2,2,4,6,7-pentamethyldihydro-benzofuran-5-sulfonyl for arginine; *tert*-butyl ether for serine; *tert*-butyloxycarbonyl for lysine. The Fmoc group was removed by using 20% piperidine in NMP. The other protecting groups were removed during cleavage of the peptide from the solid support by treatment with a TFA/triisopropylsilane/H<sub>2</sub>O solution at a 95/2.5/2.5 ratio for 2 h. After cleavage, the solid support was removed by filtration, and the filtrate was concentrated under reduced pressure. The crude peptides were precipitated from diethyl ether, washed several times with diethyl ether, and dried under reduced pressure.

RP-HPLC peptide analysis was performed on a Jupiter Proteo analytical C<sub>12</sub> column (4.6×250 mm) supplied by Phenomenex (Torrance, CA, USA), using 0.1% TFA/H<sub>2</sub>O as solvent A, and 0.1% TFA/MeCN as solvent B. The column was equilibrated with an A/B ratio of 95/5 at a flow rate of 1.0 ml/min, and the concentration of B was raised to 95% (v/v) over 14 min using gradient mode conditions. The peptide was purified on a Jupiter Proteo semipreparative C<sub>12</sub> column (10×250 mm), and the major peak in the chromatogram was collected by an automatic fraction collector. The dendrimeric SB056 was obtained with a final purity of around 95%. The monoisotopic molecular mass of the dendrimer was determined by MALDI-TOF MS (Bruker Daltonik, Bremen, Germany), using sinapinic acid as an acidic matrix. The instrument was calibrated with peptides of known molecular mass in the 1000-6000 Da range.

#### Microbial strains and culture media

Amikacin sulphate, amphotericin B, ciprofloxacin, colistin sulphate, erythromycin, ethambutol, 5-Fluorocytosine, gentamicin, polymyxin B sulphate, and vancomycin HCl, all used as controls, were purchased from Sigma-Aldrich. All compounds were dissolved in DMSO (Becton Dickinson, Franklin Lakes, NJ, USA), distilled water, or Na-phosphate buffer pH 6.0, according to CLSI guidelines (formerly NCCLS) (1), to obtain stock solutions of 10 mg/ml. All compounds were subsequently diluted in Mueller Hinton Broth (MHB; Difco Laboratories, Sparks, MD, USA), Cation-adjusted MHB (CAMHB: MHB adjusted with CaCl<sub>2</sub> and MgCl<sub>2</sub> at final concentrations of 20 mg/l and 10 mg/l, respectively), RPMI-1640 (Sigma-Aldrich), or 7H9 (Becton Dickinson) medium to obtain working solutions.

All bacterial strains used in the present study belong to the NeED Pharmaceuticals S.r.l. strain collection (see Table S1). All clinical isolates showed antibacterial resistance phenotypes and proved resistant to various

antibacterial agents of common use in nosocomial institutions. Stock cultures of Gram-positive and Gram-negative bacteria, *Candida* spp. and *Mycobacterium smegmatis* mc<sup>2</sup>155, were prepared from isolated colonies selected on Mueller Hinton Agar (MHA; Difco Laboratories), Sabouraud (Becton Dickinson) or 7H11 (Bioline, Italy) agar plates, respectively, and diluted into MHB/Sabouraud/7H9 medium to 0.2 OD<sub>625</sub>, rapidly frozen, and stored at -80 °C. In all experiments the weighed amount of SB056 was considered to be 100% potent, though it must be noted that the actual potency was approximately 65-70%, due to the presence of salts in the stock compound.

### Determination of minimal inhibitory concentrations (MIC)

MIC assays were performed by broth microdilution methodology in sterile 96-well microtiter plates (Greiner Bio-One, Monroe, NC, USA), according to CLSI procedures (2-4). Microorganisms were added at final concentration of 1x10<sup>4</sup> CFU/ml for *Candida* spp., 1-5x10<sup>6</sup> CFU/ml for *M. smegmatis* mc<sup>2</sup>155, and 1-5x10<sup>5</sup> CFU/ml for Gram-negative and Gram-positive bacteria, respectively. Plates were incubated at 37 °C and read out after 20-24 h for Gram-negative and Gram-positive bacteria, 48 h for *Candida* spp., and 72 h for *M. smegmatis* mc<sup>2</sup>155, respectively. The MIC value was defined as the lowest drug concentration causing complete suppression of visible bacterial growth.

### CD spectropolarimetry

The lipid powders (DMPC, DMPG) were dissolved in chloroform/methanol 50/50 (vol%) to get lipid stock solutions of around 14 mM. Aliquots of the stock solutions were mixed in a glass vial and thoroughly vortexed to obtain the DMPC/DMPG 1:1 mixture (molar ratio). Subsequently, the organic solvents were removed under a gentle stream of nitrogen, followed by overnight vacuum. The DMPC or DMPC/DMPG lipid film that had formed in the vial was dispersed by addition of 10 mM phosphate buffer (pH 7.0) and homogenized by vigorously vortexing for 7x1 min and by 7 freeze-thaw cycles. Afterwards, small unilamellar vesicles (SUVs) were formed by sonication of the MLVs for 5 min in a strong ultrasonic bath (UTR 200, Hielscher, Germany). To prepare the final CD samples, an aliquot of the respective peptide stock solution was added to the liposome dispersion, or to a 10 mM phosphate buffer/TFE (2,2,2-trifluoroethanol) mixture (see Supporting Material). The TFE content was varied between 0 and 90 vol% in steps of 10, and the final peptide concentration varied between 5 and 50 µM. In the liposome samples it was adjusted to 15 µM, which resulted in a peptide-to-lipid ratio of 1:100, given the lipid concentration of 1.5 mM.

CD spectra of these samples were recorded on a J-815 spectropolarimeter (JASCO, Groß-Umstadt, Germany). Measurements were performed in quartz glass cells (Suprasil, Hellma) of 1 mm path length between 260 and 185 nm at 0.1 nm intervals. Spectra were recorded at 20 °C for the phosphate buffer/TFE mixtures, and at 30 °C for the vesicle suspensions (i.e. above the lipid phase transition temperature), using a water-thermostatted rectangular cell holder. Three repeat scans at a scan-rate of 10 nm min<sup>-1</sup>, 8 s response time and 1 nm bandwidth were averaged for each sample and for the baseline of the corresponding protein-free sample. After subtracting the baseline spectra from the sample spectra, CD data were processed with the adaptive smoothing method, which is part of the Jasco Spectra Analysis software.

To calculate the mean residue ellipticities necessary for quantitative secondary structure estimation, the concentration of the stock solution of the linear monomer or the dendrimeric SB056 was carefully determined, based on the UV absorbance of the respective peptide at 280 nm (5). The absorption spectrum in the range of the tryptophan aromatic bands was recorded from 340 to 240 nm in a quartz glass half-micro-cuvette with 1 cm optical path length (Hellma), using 10 mM phosphate buffer as a blank. The concentration of the peptide stock solutions was determined from the baseline-corrected absorbance at 280 nm, using a molar extinction coefficient of 5500 l mol<sup>-1</sup> cm<sup>-1</sup> for the linear monomer, and 11000 l mol<sup>-1</sup> cm<sup>-1</sup> for dendrimeric SB056. The concentration of the CD samples was thus calculated from the respective dilution factors. Secondary structure analysis was performed using the CDSSTR program with the implemented SVD (singular value decomposition) algorithm (6,7), which is provided by the DICHROWEB on-line server (8,9). The quality of the fit between experimental and back-calculated spectrum corresponding to the derived secondary structure

fractions was assessed from the normalized root mean square deviation (NRMSD), with a value <0.1 considered as a good fit (9).

## NMR characterization

$^1\text{H}$ -NMR spectra were recorded at 298 K in 5 mm tubes on a Varian Unity-Inova spectrometer at a proton resonance frequency of 399.948 MHz. Chemical shifts are quoted relative to the methyl protons of TSP (trimethylsilyl-2,2,3,3-tetradeuteropropanoic acid, 98.0% D, Cambridge Isotope Laboratories) used as an external reference.  $^1\text{H}$  spectra were recorded using 6.2  $\mu\text{s}$  pulse ( $90^\circ$ ), 1 s delay time, 2 s acquisition time, a spectral width of 5 kHz, and 128 scans. Correlation spectroscopy (COSY) spectra were acquired over the same spectral window, using 2048 complex points and sampling each of the 256 increments with 128 scans. Phase-sensitive total correlation spectroscopy (TOCSY) spectra were collected using the same parameters as COSY, with 50 ms spin-lock time using the MLEV-17 mixing scheme.  $^1\text{H}$ - $^1\text{H}$  nuclear Overhauser effect spectroscopy (NOESY) spectra were recorded with 200 ms mixing time.  $^1\text{H}$ - $^1\text{H}$  rotating frame NOE spectroscopy (ROESY) spectra were acquired with 250 ms spin-lock using MLEV-17 mixing scheme. Suppression of the water signal was always achieved by direct saturation during the relaxation delay.

Structure calculations were performed using the simulated annealing molecular dynamics algorithm implemented in DYNAMO (<http://spin.niddk.nih.gov/NMRPipe/dynamo>). The temperature was increased to 4000 K in 1000 initialization steps, then kept constant for 4000 steps, and finally slowly decreased to 0 K during the 20000 steps cooling stage. Experimental  $^3J_{\text{HNH}\alpha}$  scalar couplings were used to restrain the backbone  $\Phi$  angles using the Karplus equation parameters reported in (10). ROE and NOE cross-peaks were classified on the basis of their relative intensity as strong, medium or weak, and an upper separation boundary of 2.7, 3.3 and 5.0  $\text{\AA}$  respectively was applied to restrain the distance between the corresponding protons; 1000 structures were computed for each one of the peptides.

## Molecular Dynamics simulations

For both the dendrimeric SB056 and for the linear monomer, 1000 structures were generated each. The respective structure featuring the lowest root mean square deviation (RMSD) from the computed average backbone conformation (amongst the 100 lowest potential energy structures) was then chosen as the starting one for Molecular Dynamics (MD) simulations.

MD simulations were performed with GROMACS (11 and references therein) on either the linear monomer or on the dendrimeric SB056, both in water and in 30 vol% TFE. The GROMOS-53A6 force field (12) was used for the peptides, TFE and ions, and the SCP model (13) for water. No NMR experimental parameters were introduced in the MD simulations. Force-field parameters for the lysine linker and the 8-aminoctanamide tail of dendrimeric SB056 were obtained with PRODRG (14), except for the charges. These were evaluated according to the RESP approach: the ligand was first optimized at the HF/6-31G(d) level up to a convergence in energy of  $10^{-5}$  AU using the Gaussian03 package (15,16). The CPCM (17) implicit solvent model was employed in order to avoid formation of intramolecular H-bonds due to the *in vacuo* conditions (18). A further restrained optimization was performed *in vacuo* using the same level of theory, and the electrostatic potential map calculated. Atomic RESP (19) charges were derived from the electrostatic potential using the *antechamber* module of the AMBER package (20). Peptides were solvated in a cubic box of 8 nm long edges. About 17000 water molecules, or about 11000 water plus 1250 TFE molecules were used for simulations in water and in 30% TFE, respectively. In the latter, the molar fraction of TFE was equal to 0.1, i.e. the same conditions as employed in the NMR experiments. Finally, chloride ions were added to the simulation boxes in order to neutralize the total charge of the system.

Before running MD simulations, 1000 steps of energy minimization were performed using the steepest descent algorithm. First, positional restraints were applied on the heavy atoms of the peptide in order to allow relaxation of the solvent molecules. Then, simulated annealing followed (2 fs time-step), with a linear increase of the temperature from 0 to 300 K in 100 steps of 10 ps each. The temperature was then maintained around 300 K for an additional 100 ps. Bonds with hydrogen atoms were constrained using the LINCS algorithm (21).

Finally, a 1 ns equilibration was performed. The production runs, after equilibration, were 100 ns long. System coordinates were recorded every 4 ps (25000 frames). All simulations were carried out in the NPT ensemble at 300 K and 1 bar. The velocity-rescale algorithm (22) with  $\tau_T=1.0$  ps was used for temperature coupling. The Berendsen (23) and Parrinello-Rahman algorithms (24,25) with  $\tau_p=1$  ps were used for pressure coupling during equilibration and the production run, respectively. A twin-range cut-off (1.0 and 1.4 nm) was used to calculate Lennard-Jones non-bonded interactions. Particle Mesh Ewald summation was used for the electrostatics with 1.0 nm cut-off.

### **Surface-pressure measurements of peptide penetration in lipid monolayers**

DMPC was dissolved in chloroform, and DMPC/DMPG (50:50, w/w) in chloroform/methanol/water (70:15:15, w/w/w), and the respective lipid solution was spread at the air/buffer (5 mM HEPES, pH 7.3) interface of a 0.5 ml subphase in a circular glass well. The surface pressure ( $\pi$ ) was measured with a Wilhelmy wire attached to a microbalance (DeltaPi, Kibron Inc., Helsinki) connected to a PC. After evaporation of the organic solvent and stabilization of the monolayers at different initial surface pressures ( $\pi_0$ ), the peptide (1  $\mu$ M, final concentration) was injected into the subphase. Peptide penetration was monitored by following the increase in surface pressure of the lipid film over the next  $\sim 36$  min. The difference between the initial surface pressure and the value observed after the penetration of peptides into the film was taken as  $\Delta\pi$ . All measurements were performed at room temperature.

## RESULTS

### CD structural analysis of the linear monomer and the dendrimeric SB056

A titration series was carried out with TFE, an apolar solvent that is well-known for its helix-inducing properties. For both peptides, CD spectra were acquired in a pure 10 mM phosphate buffer solution, and then the TFE volume fraction was increased in 10% steps up to a total of 90%. Fig. S1-A shows the corresponding CD spectra for the linear monomer, and Fig. S1-B depicts the data for the dendrimeric SB056. The spectral lineshapes in pure phosphate buffer with a minimum around 198 nm and negative ellipticities over the full spectral range indicate a typical random coil conformation for both peptides under these conditions. When the TFE content is increased, a substantial degree of helicity is induced in both systems, as seen from the general rise in ellipticities and the characteristic  $\alpha$ -helical signature with a positive band around 190 nm and two negative bands at 207 and 220 nm. Both series of spectra exhibit an isodichroic point around 202 nm, suggesting equilibrium between two populations with a mostly unordered and a mostly helical conformation, respectively. All intermediate spectra can be described by a linear combination of the extreme spectra obtained in pure phosphate buffer and in 90% TFE, as demonstrated by deconvolution with the convex constraint algorithm (CCA) (26) (data not shown).

The secondary structure composition of the linear monomer and the dendrimeric SB056 can be quantitatively estimated from the corresponding CD spectra of Fig. S1-A/B using the CDSSTR program at DICHROWEB. We obtain a helical percentage of 1% in pure phosphate buffer, and up to 80% and 64% helicity, respectively, for the monomer and dendrimer in 90% TFE (cf. Tables S7 and S8). At 30% TFE, both peptides show nearly identical secondary structures with a helicity of ~50% (plus ~13%  $\beta$ -sheet, ~12%  $\beta$ -turn, 25% unordered). Any further increase in the TFE content leads to a higher helicity in the linear monomer compared to the dendrimeric SB056. The comparative CD structure analysis of the linear monomer and the dendrimeric SB056 showed that both peptides have a mostly unordered conformation in aqueous solution. The addition of TFE eventually induces a predominantly  $\alpha$ -helical structure up to a concentration of 90%, which is more pronounced for the linear monomer (80% helix) than for the dendrimeric SB056 (64%).

## SUPPORTING REFERENCES

1. National Committee for Clinical Laboratory Standards. 2006. Performance Standards for Antimicrobial Susceptibility Testing. Approved Standard. 16th Informational Supplement. NCCLS document M100-S16, NCCLS, Wayne, PA.
2. National Committee for Clinical Laboratory Standards. 2006. Methods for Dilution Antimicrobial Susceptibility Tests for Bacteria That Grow Aerobically. Approved Standard. 7th ed. NCCLS document M7-A7, NCCLS, Wayne, PA.
3. National Committee for Clinical Laboratory Standards. 2006. Reference Methods for Broth Dilution Antifungal Susceptibility Testing of Yeasts. Approved Standard. 2nd ed. NCCLS document M27-A2, NCCLS, Wayne, PA.
4. Committee for Clinical Laboratory Standards. 2006. Susceptibility Testing of Mycobacteria, Nocardiae, and Other Aerobic Actinomycetes. Approved Standard. 2006. NCCLS document M24-A, NCCLS, Wayne, PA.
5. Pace, C. N., F. Vajdos, L. Fee, G. Grimsley, and T. Gray. 1995. How to measure and predict the molar absorption coefficient of a protein. *Protein Sci.* 11:2411-2423.
6. Johnson, W. C. 1999. Analyzing protein circular dichroism spectra for accurate secondary structures. *Proteins.* 35:307-312.
7. Sreerama, N., and R. W. Woody. 2000. Estimation of protein secondary structure from CD spectra: Comparison of CONTIN, SELCON and CDSSTR methods with an expanded reference set. *Anal. Biochem.* 287:252-260.
8. Lobley, A., L. Whitmore, and B. A. Wallace. 2002. DICHROWEB: an interactive website for the analysis of protein secondary structure from circular dichroism spectra. *Bioinformatics.* 18:211-212.
9. Whitmore, L. and B. A. Wallace. 2004. DICHROWEB, an online server for protein secondary structure analyses from circular dichroism spectroscopic data. *Nucleic Acids Res.* 32:W668-W673.
10. Habeck, M., W. Rieping, and M. Nilges. 2005. Bayesian estimation of Karplus parameters and torsion angles from three-bond scalar couplings constants. *J. Magn. Res.* 177:160-165.
11. Hess, B., C. Kutzner, D. Van der Spoel, and E. Lindahl. 2008. GROMACS 4: Algorithms for highly efficient, load-balanced, and scalable molecular simulation. *J. Chem. Theory Comput.* 4:435-447.
12. Oostenbrink, C., A. Villa, A. E. Mark, and W. F. Van Gunsteren. 2004. A biomolecular force field based on the free enthalpy of hydration and solvation: The GROMOS force-field parameter sets 53A5 and 53A6. *J. Comp. Chem.* 25:1656-1676.
13. Berendsen, H. J. C., J. P. M. Postma, W. F. Van Gunsteren, and J. Hermans. 1981. Interaction models for water in relation to protein hydration. In *Intermolecular Forces*. B. Pullman, editor. Reidel D. Publishing Company, Dordrecht. 331-342.
14. Schuettelkopf, A. W. and D. M. F. Van Aalten. 2004. PRODRG - a tool for high-throughput crystallography of protein-ligand complexes. *Acta Cryst.* D60:1355-1363.
15. Frisch, M. J., G. W. Trucks, H. B. Schlegel, G. E. Scuseria, M. A. Robb, J. R. Cheeseman, J. A. Jr. Montgomery, T. Vreven, K. N. Kudin, J. C. Burant, and J. M. Millam. 2003. GAUSSIAN. Gaussian Inc., Pittsburgh, PA.
16. Frisch, M. J., G. W. Trucks, H. B. Schlegel, G. E. Scuseria, M. A. Robb, J. R. Cheeseman, J. J. A. Montgomery, T. Vreven, K. N. Kudin, J. C. Burant, et al. 2004. Gaussian 03, Revision C.02. Gaussian Inc., Wallingford, CT.
17. Barone, V. and M. Cossi. 1998. Quantum calculation of molecular energies and energy gradients in solution by a conductor solvent model. *J. Phys. Chem. A* 102:1995-2001.
18. Vargiu, A. V., P. Ruggerone, A. Magistrato, and P. Carloni. 2008. Dissociation of minor groove binders from DNA: insights from metadynamics simulations. *Nucl. Acids Res.* 36:5910-5921.
19. Bayly, C. I., P. Cieplak, W. Cornell, and P. A. Kollman. 1993. A well-behaved electrostatic potential based method using charge restraints for deriving atomic charges: the RESP model. *J. Phys. Chem.* 97:10269-10280.
20. Case, D. A., T. A. Darden, T. E. III Cheatham, C. L. Simmerling, J. Wang, R. E. Duke, R. Luo, K. M. Merz, D. A. Pearlman, M. Crowley, et al. 2006. AMBER 9. University of California, San Francisco, CA.

21. Hess, B., H. Bekker, H. J. C. Berendsen, and J. G. E. M. Fraaije. 1997. LINCS: a linear constraint solver for molecular simulations. *J. Comp. Chem.* 18:1463-1472.
22. Bussi, G., D. Donadio, and M. Parrinello. 2007. Canonical sampling through velocity rescaling. *J. Chem. Phys.* 126:014101.
23. Berendsen, H. J. C., J. P. M. Postma, W. F. Van Gunsteren, A. Di Nola, and J. R. Haak. 1984. Molecular dynamics with coupling to an external bath. *J. Chem. Phys.* 81:3684-3690.
24. Parrinello, M., and A. Rahman. 1981. Polymorphic transitions in single crystals: A new molecular dynamics method. *J. Appl. Phys.* 52:7182-7190.
25. Nosé, S., and M. L. Klein. 1976. Constant pressure molecular dynamics for molecular systems. *Mol. Phys.* 50:1055-1076.
26. Perczel, A., M. Hollosi, G. Tusnady, and G. D. Fasman. 1991. Convex constraint analysis: a natural deconvolution of circular dichroism curves of proteins. *Protein Eng.* 4:669-679.
27. Zhao, H. X., A. C. Rinaldi, A. Di Giulio, M. Simmaco, and P. K. J. Kinnunen. 2002. Interactions of the antimicrobial peptides temporins with model biomembranes. Comparison of temporins B and L. *Biochemistry.* 41:4425-4436.
28. Coccia, C., A. C. Rinaldi, V. Luca, D. Barra, A. Bozzi, A. Di Giulio, E. C. I. Veerman, and M. L. Mangoni. 2011. Membrane interaction and antibacterial properties of two mildly cationic peptide diastereomers, bombinins H2 and H4, isolated from *Bombina* skin. *Eur. Biophys. J.* 40:577-588.

## Figure captions

FIGURE S1 CD spectra of the linear monomer (A) and the dendrimeric SB056 (B) in a titration series with TFE. Starting from a 10 mM phosphate buffer, the percentage of TFE was varied between 0 and 90 vol% in steps of 10. The spectra indicate a transition from a mostly irregular conformation to a predominantly helical structure.

FIGURE S2 Sequential ROEs/NOEs observed by <sup>1</sup>H-NMR for the linear monomer and the dendrimeric SB056 in 30% TFE (A). The NOESY HN-Ha region is also shown for the linear (B) and the dendrimeric peptide (C).

FIGURE S3 <sup>1</sup>H-NMR derived backbone RMSD values for the linear monomer (A) and dendrimeric SB056 (B) from a starting structure in 30% TFE.

FIGURE S4 Residue RMSF values in pure water and in 30% TFE for the linear monomer (A) and the dendrimeric SB056 (B). In (B), the sequence reported on the left of the linker corresponds to the peptide branch linked to the  $\alpha$ -amino group of the lysine linker, while the sequence reported on the right corresponds to the branch linked to the  $\epsilon$ -amino group of the lysine linker. The scale is different in the two graphs, in order to emphasize the role of the solvent.

FIGURE S5 Backbone  $\Phi$  and  $\Psi$  angle probability distribution of the linear monomer. (A)  $\Phi$  angles in water, (B)  $\Psi$  angles in water, (C)  $\Phi$  angles in 30% TFE, (D)  $\Psi$  angles in 30% TFE.

FIGURE S6 Backbone  $\Phi$  and  $\Psi$  angle probability distribution of dendrimeric SB056. (A) chain-A  $\Phi$  angles in water, (B) chain-B  $\Phi$  angles in water, (C) chain-A  $\Psi$  angles in water, (D) chain-B  $\Psi$  angles in water, (E) chain-A  $\Phi$  angles in 30% TFE, (F) chain-B  $\Phi$  angles in 30% TFE, (G) chain-A  $\Psi$  angles in 30% TFE, (H) chain-B  $\Psi$  angles in 30% TFE. Chain-A corresponds to the peptide branch linked to  $\alpha$ -amino group of the lysine linker; chain-B corresponds to the branch linked to  $\epsilon$ -amino group of the lysine linker.

FIGURE S7 Monolayer penetration kinetics. Typical kinetics of surface pressure increase related to SB056 (A;  $\pi_0 = 8.8$ , with 1.0  $\mu$ M peptide) and its linear monomer (B;  $\pi_0 = 9.1$ , with 1.0  $\mu$ M) penetration into a DMPC/DMPG (50:50, w/w) film are shown as representative of general trends. X-axis shows elapsed time



(sec). Peptide injection into the subphase took place at  $\approx 200$  sec (arrow). Similar trends were recorded also for the penetration of SB056 and its linear monomer into a DMPC monolayer, respectively (not shown). (C) Insertion of temporin L into a SOPC/POPG ( $X_{\text{POPG}} = 0.2$ ) monolayer at the initial surface pressure of 15.5 mN/m. The addition of the peptide (0.3  $\mu\text{M}$  final concentration) is marked by arrow (reproduced with permission from 27). (D) Kinetics of surface pressure increase related to the penetration of bombinin H4 into a PE/PG monolayer ( $\pi_0 = 14.2$ , with 1.0  $\mu\text{M}$  peptide) (reproduced with permission from 28).

**Table S1 Strains used in the present study**

	<b>Microorganism</b>	<b>Code</b>	<b>Affiliation</b>
<b>Gram-positive bacteria</b>	<i>Enterococcus faecalis</i>	ATCC29212	American Type Culture Collection
		ND001907	San Donato Hospital, Italy, 2007
		ND005607	San Donato Hospital, Italy, 2007
	<i>Enterococcus faecium</i>	ND006707	San Donato Hospital, Italy, 2007
	<i>Staphylococcus aureus</i>	ND004007	San Donato Hospital, Italy, 2007
	<i>Staphylococcus epidermidis</i>	ND006307	San Donato Hospital, Italy, 2007
<b>Gram-negative bacteria</b>	<i>Acinetobacter baumannii</i>	ND000407	San Donato Hospital, Italy, 2007
		ND015107	San Raffaele Hospital, Italy, 2007
		ND019707	San Donato Hospital, Italy, 2007
	<i>Enterobacter cloacae</i>	ND000507	San Donato Hospital, Italy, 2007
		ND001607	San Donato Hospital, Italy, 2007
		ND001807	San Donato Hospital, Italy, 2007
		ND011807	San Donato Hospital, Italy, 2007
		ND012807	San Donato Hospital, Italy, 2007
		ND013307	San Raffaele Hospital, Italy, 2007
	<i>Escherichia coli</i>	ATCC25922	American Type Culture Collection
		L47	Smith Kline and French Laboratories, 1963
		ND002907	San Donato Hospital, Italy, 2007
		ND005207	San Donato Hospital, Italy, 2007
		ND005807	San Donato Hospital, Italy, 2007
		ND007307	San Donato Hospital, Italy, 2007
		ND008007	San Donato Hospital, Italy, 2007
		ND010307	San Donato Hospital, Italy, 2007
		ND014807	San Raffaele Hospital, Italy, 2007
		ND015307	San Raffaele Hospital, Italy, 2007
		ND016307	San Raffaele Hospital, Italy, 2007
		ND016707	San Raffaele Hospital, Italy, 2007
		ND020107	San Donato Hospital, Italy, 2007
	<i>Klebsiella pneumoniae</i>	ND003007	San Donato Hospital, Italy, 2007
		ND003407	San Donato Hospital, Italy, 2007
		ND006807	San Donato Hospital, Italy, 2007
		ND007507	San Donato Hospital, Italy, 2007
		ND008307	San Donato Hospital, Italy, 2007
		ND012407	San Donato Hospital, Italy, 2007
		ND013107	San Donato Hospital, Italy, 2007
	<i>Proteus mirabilis</i>	ND000107	San Donato Hospital, Italy, 2007
		ND001407	San Donato Hospital, Italy, 2007
		ND009607	San Donato Hospital, Italy, 2007
	<i>Pseudomonas aeruginosa</i>	ATCC10145,L4	American Type Culture Collection
		ATCC27853	American Type Culture Collection
		ND000207	San Donato Hospital, Italy, 2007
		ND000307	San Donato Hospital, Italy, 2007
		ND000707	San Donato Hospital, Italy, 2007
		ND000907	San Donato Hospital, Italy, 2007
		ND001507	San Donato Hospital, Italy, 2007
		ND002207	San Donato Hospital, Italy, 2007
ND005307		San Donato Hospital, Italy, 2007	
ND006107	San Donato Hospital, Italy, 2007		

	<b>Microorganism</b>	<b>Code</b>	<b>Affiliation</b>
<b>Gram-negative bacteria</b>	<i>Pseudomonas aeruginosa</i>	ND007707	San Donato Hospital, Italy, 2007
		ND009807	San Donato Hospital, Italy, 2007
		ND010207	San Donato Hospital, Italy, 2007
		ND010907	San Donato Hospital, Italy, 2007
		ND011007	San Donato Hospital, Italy, 2007
		ND011607	San Donato Hospital, Italy, 2007
		ND012707	San Donato Hospital, Italy, 2007
		ND020007	San Donato Hospital, Italy, 2007
		ND020207	San Donato Hospital, Italy, 2007
	<i>Serratia marcescens</i>	ND015207	San Raffaele Hospital, Italy, 2007
<i>Stenotrophomonas maltophilia</i>	ND006507	San Donato Hospital, Italy, 2007	
<b>Candida spp.</b>	<i>Candida albicans</i>	ATCC90028	American Type Culture Collection
	<i>Candida krusei</i>	ATCC6258	American Type Culture Collection
	<i>Candida parapsilosis</i>	ATCC22019	American Type Culture Collection
<b>Mycobacteria spp.</b>	<i>Mycobacterium smegmatis</i>	ATCC700084 (mc <sup>2</sup> 155)	American Type Culture Collection

**Table S2 Activity of SB056 against Gram-negative bacteria**

Microorganism	Strain	MIC ( $\mu\text{g/ml}$ )							
		SB056	CL	PB	AMI	CIP	ERY	GEN	RIF
<i>Acinetobacter baumannii</i> (N = 3)	ND000407	4	1	1	16	>16	32	>16	/
	ND015107	4	0.5	0.25	>32	32	32	>64	2
	ND019707	8	1	1	/	/	/	>128	4
	Range	4-8	0.5-1	0.25-1	$\geq 16$	>16	32	>16	2-4
	ND000507	4	1	1	/	128	/	>128	8
<i>Enterobacter cloacae</i> (N = 6)	ND001607	8	0.5	1	1	>16	>128	>16	/
	ND001807	4	1	0.5	/	/	/	0.25	8
	ND011807	8	1	1	$\leq 1$	>64	>128	>128	32
	ND012807	8	0.5	0.5	1	$\leq 0.5$	$\leq 0.5$	>128	32
	ND013307	4	0.5	0.5	8	4	>64	>128	>64
	Range	4-8	0.5-1	0.5-1	$\leq 1-8$	$\leq 0.5-128$	$\leq 0.5->128$	$0.25->128$	$8->64$
	L47	2	1	1	1	$\leq 0.5$	64	2	8
	ND002907	4	2	0.5	/	64	/	128	8
	ND005207	4	0.5	0.5	/	128	/	64	4
	ND005807	8	1	1	8	64	>128	>128	8
<i>Escherichia coli</i> (N = 11)	ND008007	4	0.5	0.5	2	$\leq 0.125$	32	1	/
	ND010307	8	1	1	16	>64	>128	4	8
	ND014807	4	0.25	0.5	2	32	16	64	4
	ND015307	4	2	2	16	>64	64	2	8
	ND016307	8	1	1	64	64	>128	32	32
	ND016707	4	0.5	0.25	4	>64	64	>128	4
	ND020107	8	1	1	4	32	128	4	16
	Range	2-8	0.25-2	0.25-2	1-64	$\leq 0.125-128$	$16->128$	$1->128$	$4-32$
	ND003007	16	1	1	4	/	64	16	16
	ND003407	8	2	1	16	>16	>128	>16	/
	<i>Klebsiella pneumoniae</i> (N = 7)	ND006807	4	0.5	0.25	/	0.06	/	2
ND007507		16	1	4	>16	>16	>128	>16	/
ND008307		16	0.5	0.5	/	0.06	/	1	32
ND012407		8	1	1	2	$\leq 0.5$	$\leq 0.5$	64	16
ND013107		8	1	1	2	$\leq 0.5$	$\leq 0.5$	64	16
Range		4-16	0.5-2	0.25-4	$2->16$	$0.006->16$	$\leq 0.5->128$	$1-64$	$16-32$
ND000107		>128	>8	>8	8	4	>128	>128	4
<i>Proteus mirabilis</i> (N=3)	ND001407	32	>16	16	4	16	>128	>128	>128
	ND009607	>128	>16	>16	8	>64	>128	>128	128
	Range	$32->128$	>8	>8	4-8	$4->64$	>128	>128	$4->128$
<i>Pseudomonas aeruginosa</i> (N = 18)	ATCC10145	16	1	1	2	$\leq 0.5$	128	1	16
	ATCC27853	16	1	1	2	0.25	128	1	/
	ND000207	16	2	2	>16	16	>128	>16	/
	ND000307	8	2	1	32	16	32	2	4
	ND000707	16	1	1	>32	32	16	>128	16
	ND000907	16	2	2	128	32	>128	16	16
	ND001507	8	2	2	4	16	>128	>128	>128
	ND002207	16	2	1	4	64	>128	>128	16
	ND005307	8	1	0.5	/	/	/	/	16
	ND006107	8	1	1	128	32	>128	8	16
	ND007707	16	2	1	/	32	/	16	32
	ND010207	16	1	1	8	64	>64	>128	16
ND010907	4	0.5	0.5	4	4	128	2	/	

	ND011007	16	1	1	2	/	32	>128	16
	ND011607	8	1	1	4	32	>128	>128	32
	ND012707	16	2	2	2	≤0.5	128	≤1	16
	ND020007	32	2	2	4	≤0.5	>128	≤1	32
	ND020207	32	1	1	/	32	/	>64	16
	Range	4-32	0.5-2	0.5-2	2-128	0.25-64	32->128	1->128	4->128
<i>Serratia marcescens</i>	ND015207	>128	>8	>8	4	≤0.05	>128	4	32
<i>Stenotrophomonas maltophilia</i>	ND006507	8	1	1	4	2	>128	2	/

Abbreviations: CL, colistin; PB, polymyxin B; AMI, amikacin; CIP, ciprofloxacin; ERY, erythromycin; GEN, gentamicin; RIF, rifampicin

**Table S3 Activity of SB056 against Gram-positive bacteria**

Microorganism	Strain	MIC ( $\mu\text{g/ml}$ )				
		SB056	CL	PB	GEN	VAN
<i>Enterococcus faecalis</i>	ATCC29212	32	>128	>128	16	2
	ND001907	64	>128	>128	>128	0.5
	ND005607	64	>128	>128	8	0.5
<i>Enterococcus faecium</i>	ND006707	8	>128	>128	>128	0.5
<i>Staphylococcus aureus</i>	ND004007	32	>128	128	0.5	0.25
<i>Staphylococcus epidermidis</i>	ND006307	8	128	32	32	2

Abbreviations: CL, colistin; PB, polymyxin B; GEN, gentamicin; VAN, vancomycin

**Table S4 Activity of SB056 against *Candida* spp. and *Mycobacterium smegmatis* mc<sup>2</sup>155**

Microorganism	Strain	MIC ( $\mu\text{g/ml}$ )				
		SB056	AMPHO	5FC	CIP	EMB
<i>Candida albicans</i>	ATCC90028	>128	2	0.5	/	/
<i>Candida krusei</i>	ATCC6258	>128	2	32	/	/
<i>Candida parapsilosis</i>	ATCC22019	>128	2	2	/	/
<i>Mycobacterium smegmatis</i> mc <sup>2</sup> 155	ATCC700084	64	/	/	0.25	0.25

Abbreviations: AMPHO, amphotericin B; 5FC, 5-fluorocytosine; CIP, ciprofloxacin; EMB, ethambutol;

**Table S5 Activity of SB056 compared to its linear monomer against reference bacteria**

Microorganism	No. of tested strains	MIC ( $\mu\text{g/ml}$ )	
		SB056	linear monomer
<i>Escherichia coli</i>	11	2-8	64-128
<i>Pseudomonas aeruginosa</i>	18	4-32	64-128
<i>Klebsiella pneumoniae</i>	7	4-16	128-256
<i>Staphylococcus aureus</i>	1	32	512



**Table S6 Secondary structure fractions of the linear and dendrimeric SB056 peptides in SUVs composed of DMPC and DMPC/DMPG (1:1), evaluated from the CD spectra using CDSSTR (6)**

Sample	Fraction of secondary structure				NRMSD
	$\alpha$ -helix	$\beta$ -sheet	$\beta$ -turn	unordered	
Monomer in DMPC	0.01	0.08	0.05	0.83	0.026
Monomer in DMPC/DMPG 1:1	0.05	0.34	0.22	0.38	0.022
Dendrimer in DMPC	0.04	0.13	0.09	0.74	0.009
Dendrimer in DMPC/DMPG 1:1	-0.05	0.47	0.28	0.26	0.049

Abbreviations: NRMSD, normalized root mean square deviation between the calculated and experimental CD spectra

**Table S7 Secondary structure fractions of the linear monomer peptide in 10 mM phosphate buffer/TFE mixtures, evaluated from the CD spectra using CDSSTR (6)**

Sample	Fraction of secondary structure				NRMSD
	$\alpha$ -helix	$\beta$ -sheet	$\beta$ -turn	unordered	
TFE/pB 0:100	0.01	0.07	0.06	0.85	0.008
TFE/pB 10:90	0.02	0.08	0.06	0.82	0.008
TFE/pB 20:80	0.19	0.21	0.18	0.42	0.011
<b>TFE/pB 30:70</b>	<b>0.50</b>	<b>0.14</b>	<b>0.11</b>	<b>0.25</b>	<b>0.010</b>
TFE/pB 40:60	0.59	0.10	0.08	0.23	0.007
TFE/pB 50:50	0.62	0.10	0.07	0.20	0.007
TFE/pB 60:40	0.58	0.12	0.09	0.21	0.006
TFE/pB 70:30	0.61	0.09	0.07	0.22	0.008
TFE/pB 80:20	0.67	0.08	0.07	0.18	0.005
TFE/pB 90:10	0.80	0.05	0.03	0.12	0.008

Abbreviations: pB, phosphate buffer; NRMSD, normalized root mean square deviation between the calculated and experimental CD spectra.

**Table S8 Secondary structure fractions of the dendrimeric SB056 peptide in 10 mM phosphate buffer/TFE mixtures, evaluated from the CD spectra using CDSSTR (6)**

Sample	Fraction of secondary structure				
	$\alpha$ -helix	$\beta$ -sheet	$\beta$ -turn	unordered	NRMSD <sup>a)</sup>
TFE/pB 0:100	0.01	0.15	0.09	0.73	0.010
TFE/pB 10:90	0.05	0.16	0.12	0.67	0.011
TFE/pB 20:80	0.36	0.16	0.14	0.34	0.015
<b>TFE/pB 30:70</b>	<b>0.51</b>	<b>0.11</b>	<b>0.13</b>	<b>0.25</b>	<b>0.010</b>
TFE/pB 40:60	0.54	0.12	0.08	0.25	0.007
TFE/pB 50:50	0.55	0.11	0.12	0.22	0.011
TFE/pB 60:40	0.56	0.10	0.12	0.22	0.007
TFE/pB 70:30	0.58	0.12	0.10	0.21	0.007
TFE/pB 80:20	0.61	0.12	0.08	0.20	0.005
TFE/pB 90:10	0.64	0.11	0.06	0.21	0.005

Abbreviations: pB, phosphate buffer; NRMSD, normalized root mean square deviation between the calculated and experimental CD spectra

**Table S9 Protons chemical shift observed for dendrimeric SB056 and the linear peptide in pure water (with 10 % D<sub>2</sub>O) and in 30 % TFE**

Residue	Protons group	Chemical shift <sup>a</sup> (ppm)				
		Random-coil value <sup>b</sup>	Linear SB056		SB056	
			90:10 H <sub>2</sub> O:D <sub>2</sub> O	70:30 H <sub>2</sub> O:TFE	90:10 H <sub>2</sub> O:D <sub>2</sub> O	70:30 H <sub>2</sub> O:TFE
W	HN	8.09	6.64	6.71	---	---
	HC $\alpha$	4.7	4.32	4.38	4.08	4.35
	HC $\beta$	3.32	3.42	3.5	3.28	3.48
		3.19	3.35	3.4		3.36
	HN1	10.22	10.24	10.25	10.18	10.18
	HC2	7.24	7.31	7.37	7.27	7.33
	HC4	7.65	7.58	7.66	7.57	7.64
	HC5	7.17	7.15	7.21	7.13	7.16
	HC6	7.24	7.26	7.31	7.24	7.27
HC7	7.5	7.52	7.57	7.5	7.52	
K <sup>c</sup>	HN	8.41	8.35	8.41	8.07	8.44
	HC $\alpha$	4.36	4.25	4.35	4.19	4.32
	HC $\beta$	1.85	1.71	1.8	1.71	1.79
		1.76	1.65	1.74	1.36	
	HC $\gamma$	1.45	1.38	1.38	1.36	1.36
	HC $\delta$	1.7	1.63	1.69	1.66	1.69
	HC $\epsilon$	3.02	2.95	3.01	2.94	2.98
	HN $\zeta$	7.52	7.51	---	---	---
K <sup>c</sup>	HN	8.41	8.27	8.24	8.07	8.24
	HC $\alpha$	4.36	4.16	4.3	4.16	4.23
	HC $\beta$	1.85	1.71	1.8	1.71	1.79
		1.76	1.65	1.74	1.36	
	HC $\gamma$	1.45	1.31	1.38	1.16	1.36
	HC $\delta$	1.7	1.63	1.69	1.56	1.69
	HC $\epsilon$	3.02	2.95	3.01	2.89	2.98
	HN $\zeta$	7.52	7.51	---	---	---
I	HN	8.19	8.2	8.02	8.16	7.92
	HC $\alpha$	4.23	4.12	4.23	4.12	4.16
	HC $\beta$	1.9	1.81	1.88	1.81	1.85
	HC $\gamma$ 1	1.48	1.44	1.62	1.46	1.6
		1.19	1.17	1.22	1.16	1.19
	HC $\gamma$ 2	0.95	0.87	0.94	0.86	0.9
	HC $\delta$ 1	0.89	0.84	0.89	0.82	0.86
R <sup>d</sup>	HN	8.27	8.45	8.3	8.46	8.16
	HC $\alpha$	4.38	4.34	4.44	4.34	4.35
	HC $\beta$	1.89	1.79	1.88	1.79	1.85
		1.79	1.72	1.78		
	HC $\gamma$	1.7	1.59	1.66	1.72	1.79
	HC $\delta$	3.32	3.17	3.22	3.16	3.19
	HN $\epsilon$	7.17	7.15	7.22	7.85	7.64
	HN $\eta$	6.62	7.53	7.51	7.5	7.21

V	HN	8.44	8.18	7.97	8.18	7.88
	HC $\alpha$	4.18	4.08	4.19	4.07	4.08
	HC $\beta$	2.13	2.02	2.11	2.01	2.07
	HC $\gamma$	0.97 0.94	0.92	0.97	0.91	0.94
R <sup>d</sup>	HN	8.27	8.44	8.27	8.46	8.16
	HC $\alpha$	4.38	4.34	4.4	4.34	4.35
	HC $\beta$	1.89	1.79	1.88	1.79	1.85
		1.79	1.72	1.78		
	HC $\gamma$	1.7	1.55	1.61	1.72	1.79
	HC $\delta$	3.32	3.17	3.22	3.16	3.19
	HN $\epsilon$	7.17	7.15	7.22	7.85	7.64
		7.53	7.51	7.5		
	HN $\eta$	6.62	7.05	7	6.78	7.21
L	HN	8.42	8.41	8.24	8.39	8.13
	HC $\alpha$		7.05	7	6.78	
		4.38	4.36	4.44	4.36	4.35
	HC $\beta$	1.65	1.61	1.67	1.61	1.68
	HC $\gamma$	1.64	1.61	1.67	1.61	1.68
		0.94	0.92	0.97	0.91	0.88
	HC $\delta$	0.9	0.86	0.92	0.85	0.86
S <sup>e</sup>	HN	8.38	8.3	8.12	8.31	8.03 ; 7.98
	HC $\alpha$	4.5	4.41	4.5	4.4	4.43 ; 4.40
	HC $\beta$	3.88	3.87	3.93	3.87	3.86
			3.82	3.89	3.82	
HO $\gamma$	---	---	---	---	---	
A <sup>f</sup>	HN	8.25	8.33	8.24	---	8.07 ; 7.99
	HC $\alpha$	4.35	4.31	4.35	4.30 ; 4.25	4.32 ; 4.30

	HC $\beta$	1.39	1.39	1.46	1.38 ; 1.35	1.43 ; 1.39
	H <sub>2</sub> N-terminus	---	6.64	6.71	---	---
K linker	HN	---	---	---	---	7.83
	HC $\alpha$	---	---	---	4.34	4.2
	HC $\beta$	---	---	---	1.59	1.79
	HC $\gamma$	---	---	---	1.28	1.36
	HC $\delta$	---	---	---	1.48	1.69
	HC $\epsilon$	---	---	---	3.16	2.98
	HN $\zeta$	---	---	---	---	---
lipidic tail <sup>g</sup>	HN8	---	---	---	---	7.52
	HC8	---	---	---	2.23	3.19
	HC7	---	---	---	1.55	1.57
	HC6	---	---	---	1.28	1.31
	HC5	---	---	---	1.28	1.31
	HC4	---	---	---	1.28	1.31
	HC3	---	---	---	1.28	1.31
	HC2	---	---	---	1.47	1.5
	HN1	---	---	---	---	---

<sup>a</sup> chemical shifts are referred to the resonance of TSP methyl groups

<sup>b</sup> Wüthrich K., "NMR of Proteins and Nucleic Acids", Ed.: J.Wiley & Sons Inc., Chichester - UK, 1986

<sup>c</sup> two lysines were always distinguishable on the basis of chemical shifts but, in this work, it was not possible to assigned their resonances unambiguously to the first or the second one along the peptides sequence

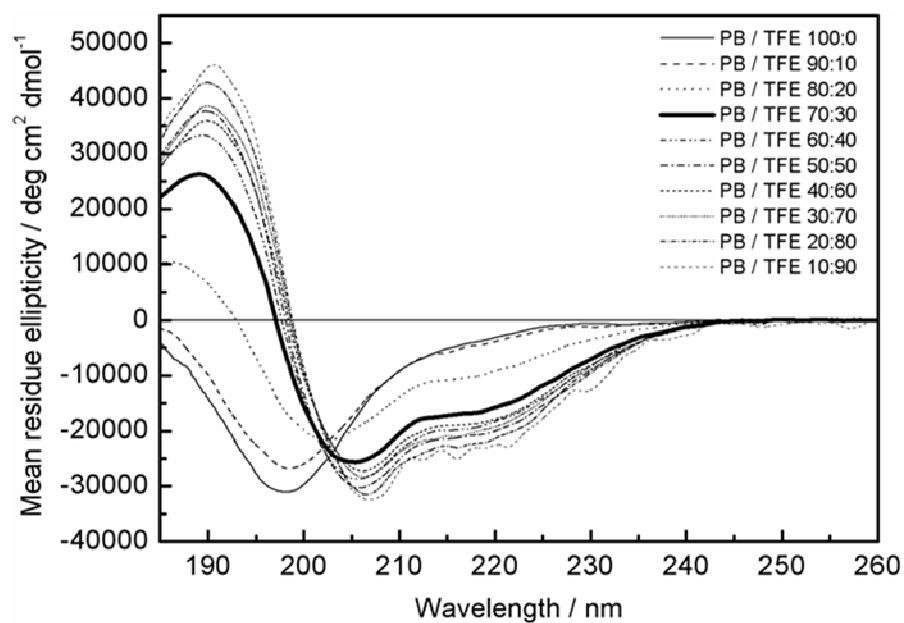
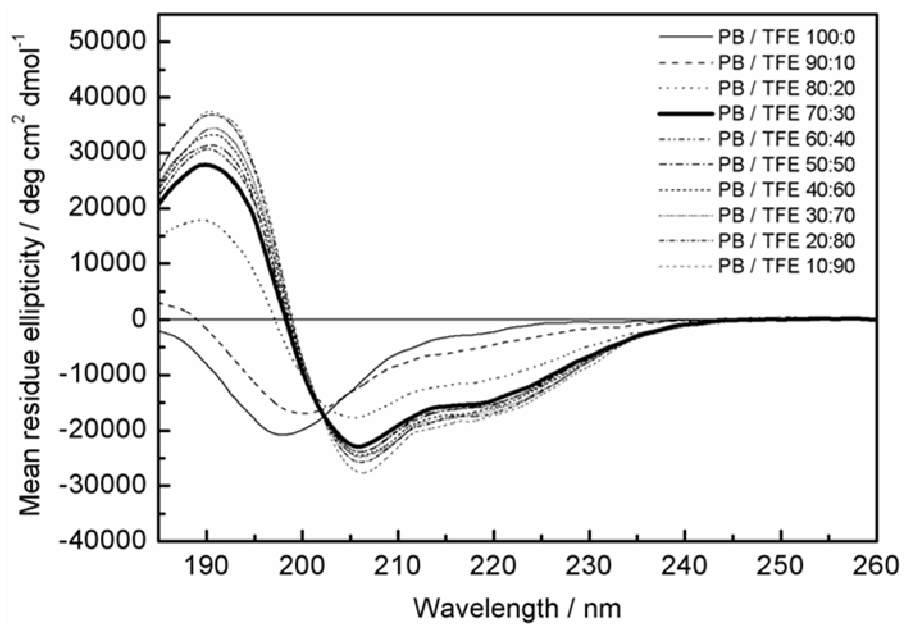
<sup>d</sup> two arginine were always distinguishable on the basis of chemical shifts and resonances could be assigned unambiguously to R5 and R7 on the basis of bidimensional NOESY and/or ROESY experiments

<sup>e</sup> serines in the two branches of the dendrimeric SB056 were distinguishable only in the water/TFE mixture

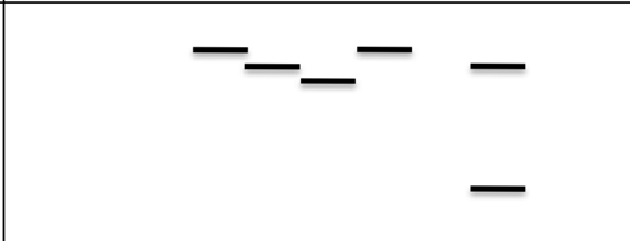

<sup>f</sup> alanines in the two branches of the dendrimeric SB056 were distinguishable both in the water/TFE mixture and in water

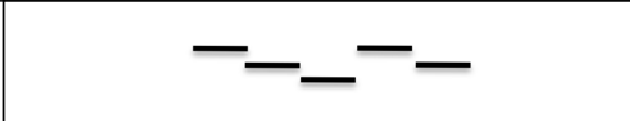

<sup>g</sup> lipidic tail of the dendrimeric SB056 is a 8-aminooctanamide

# Figure S1

**A****B**

**Figure S2**

<i>lin-SB056</i>	W K K I R V R L S A
$d_{\alpha N}(i,i+1)$	
$d_{\beta N}(i,i+1)$	
$d_{\alpha N}(i,i+2)$	

<i>SB056</i>	W K K I R V R L S A
$d_{\alpha N}(i,i+1)$	
$d_{\alpha N}(i,i+2)$	



**Figure S3**

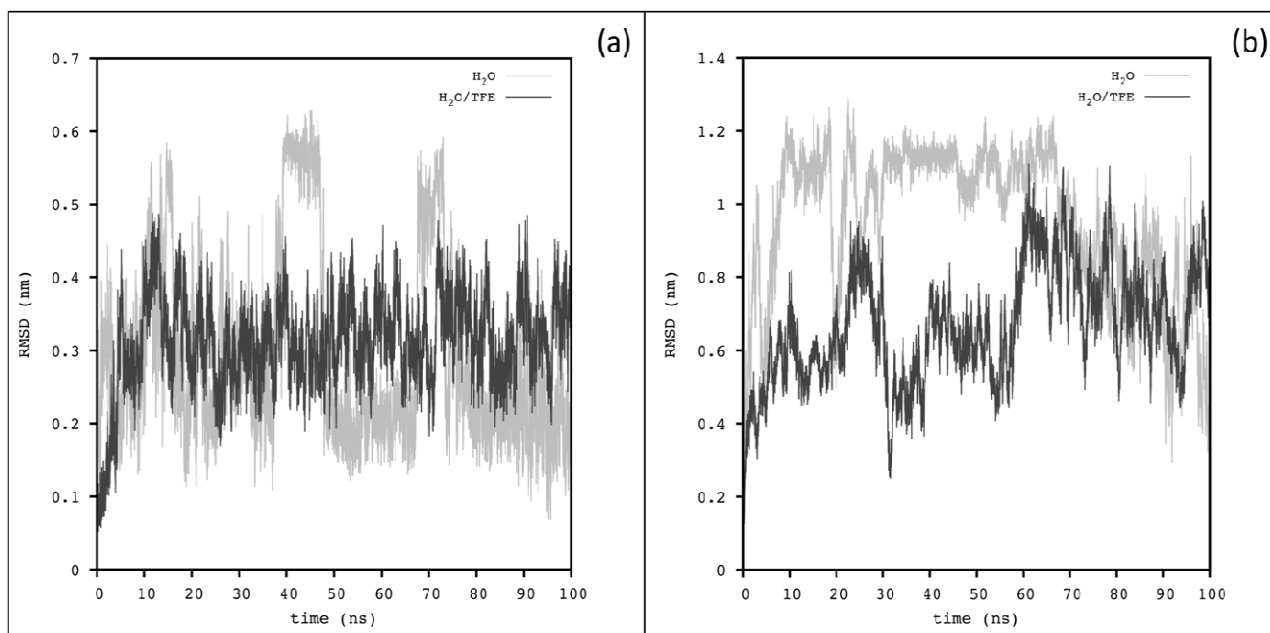


**Figure S4**

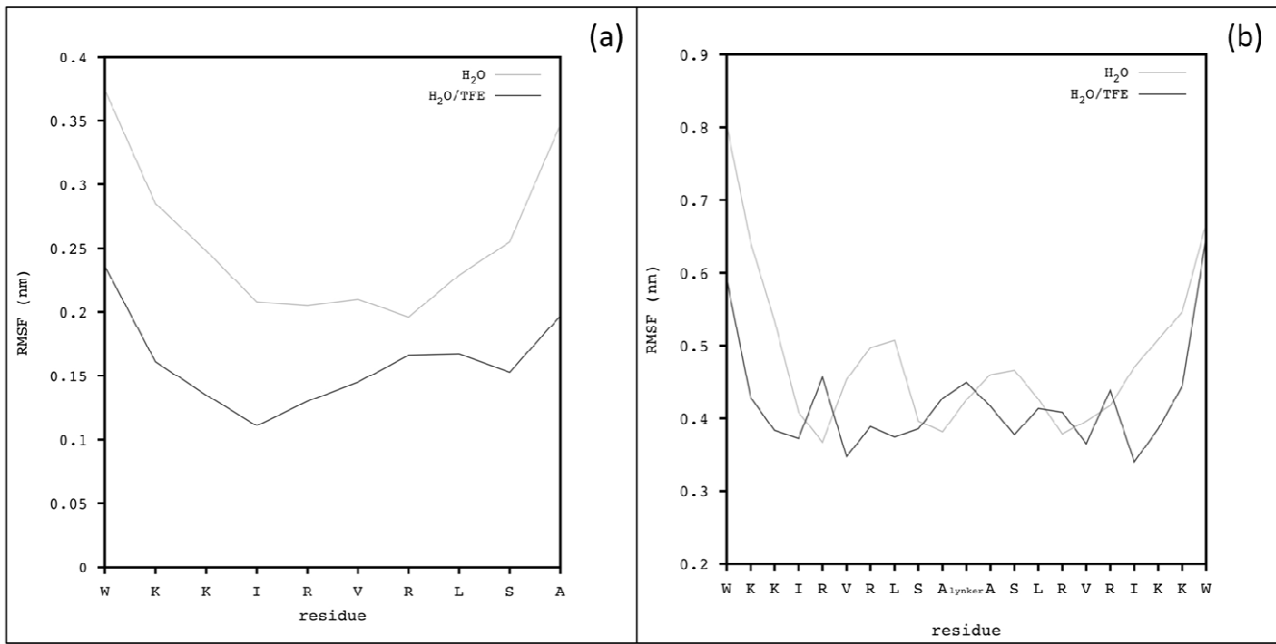


**Figure S5**

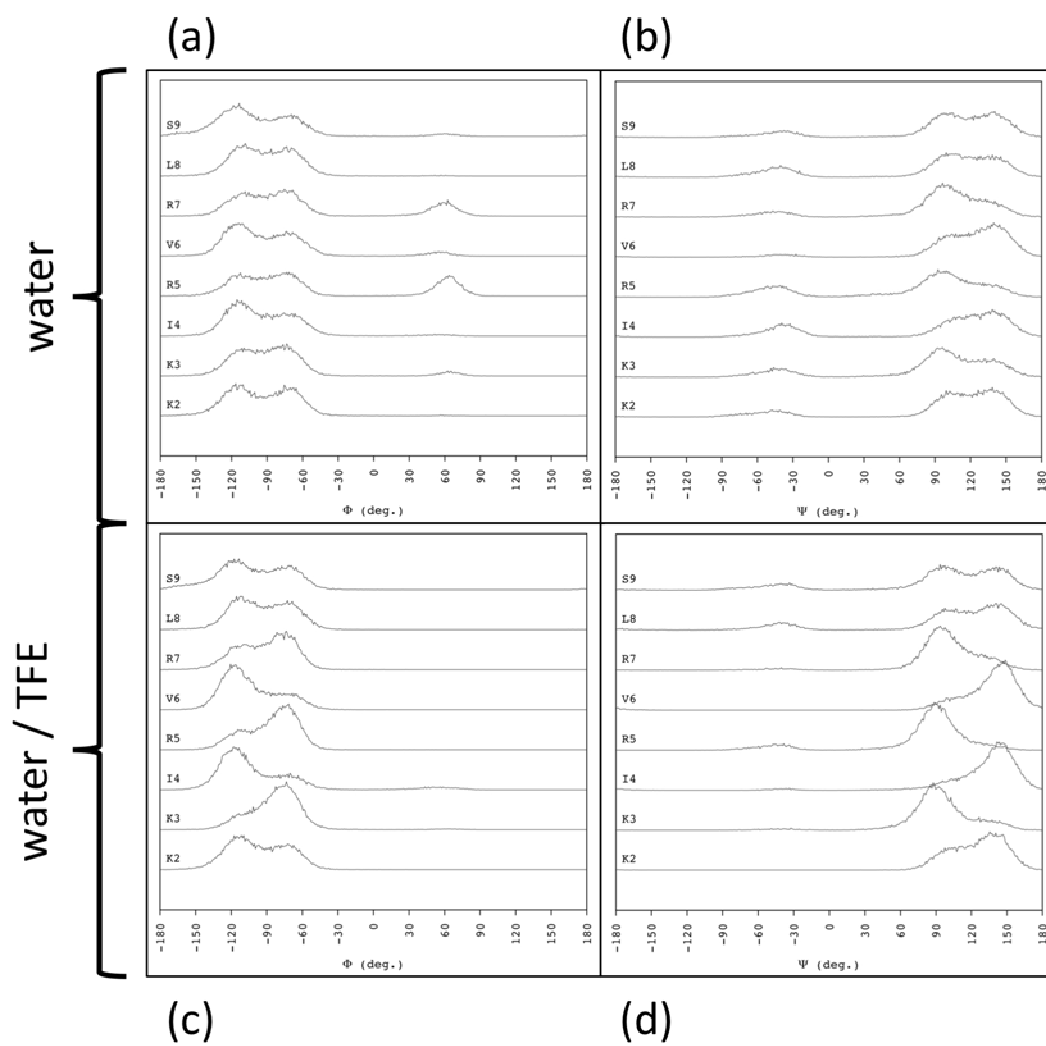


# Figure S6

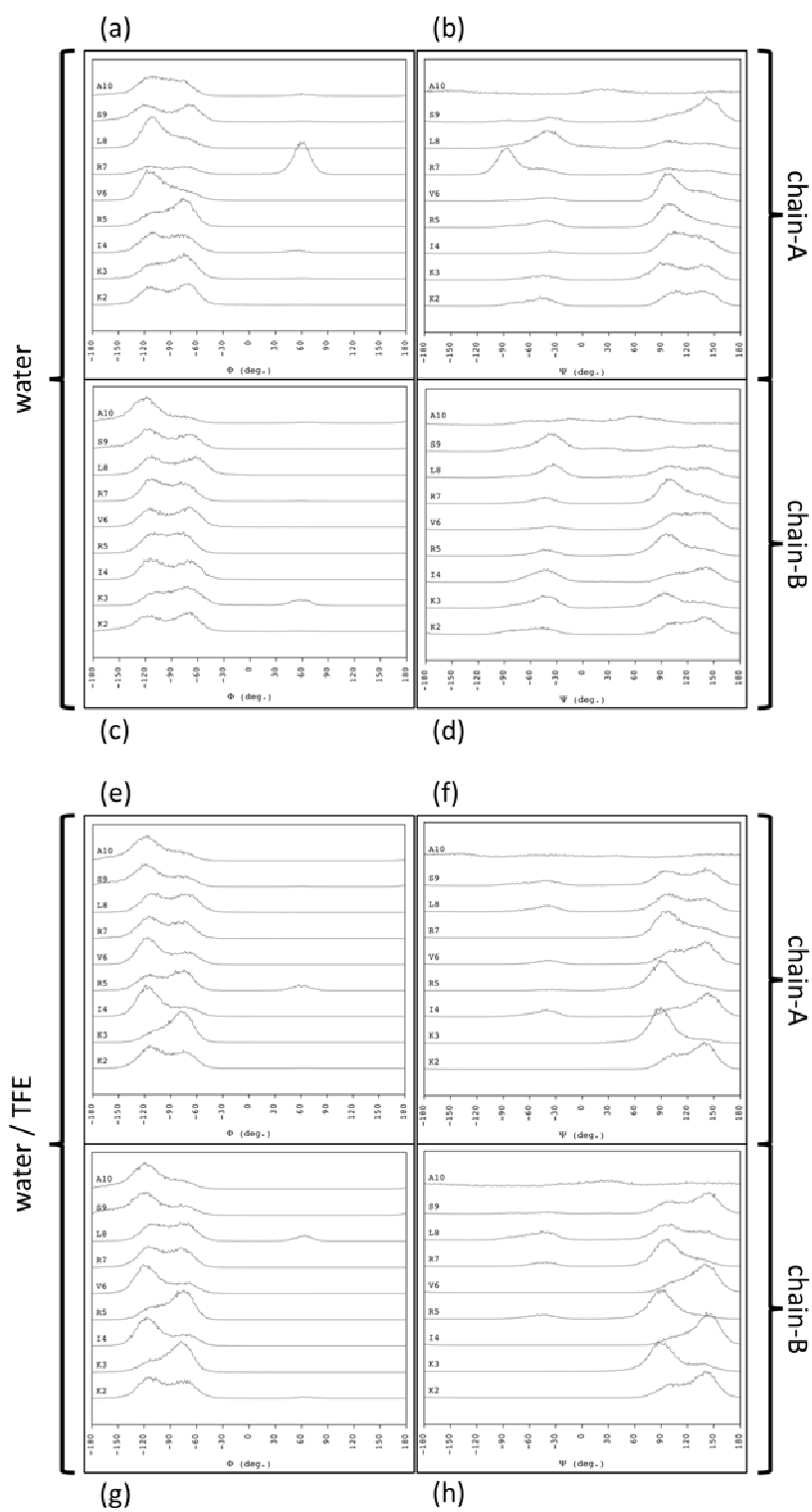


**Figure S7**

